NMPC-based guidance and control for autonomous high-thrust non-coplanar LEO-GEO missions

IAC-22-C1.3.8.73465

NMPC-based guidance and control for autonomous high-thrust non-coplanar LEO-GEO missions

M. Pagone[a]*, M. Boggio[a], C. Novara[a], L. Massotti[b]

[a] *Department of Electronics and Telecommunications, Politecnico di Torino, Corso Duca degli Abruzzi, 24, 10129, Torino, Italy*, michele.pagone@polito.it, mattia.boggio@polito.it, carlo.novara@polito.it
[b] *ESA/ESTEC, Keplerlaan 1, 2201 AZ Noordwijk, The Netherland*, luca,massotti@esa.int
* Corresponding Author

Abstract
This paper presents a novel Nonlinear Model Predictive Control strategy for autonomous guidance and control in high-thrust quasi-impulsive maneuvers. A sparse-in-time thrust behavior is promoted within the performance index. Sparsity and bang-bang behavior are indeed important features in view of the propellant consumption reduction. The guidance and control algorithm takes advantage of the so-called Modified Equinoctial Orbital Elements, which also allow a reduction of potential numerical singularities with respect to the standard Keplerian elements. A case study is presented, regarding a non-coplanar Low Earth Orbit - Geostationary Orbit transfer mission. In the case study, we show the effectiveness of the proposed strategy, compared to other approaches derived from classical astrodynamics.
Keywords: Orbital, High-thrust, Guidance, Control, Spacecraft, GTO

Nomenclature
ΔV: Delta-V
μ: Earth's planetary constant
γ: Flight path angle
g_0: Earth's gravity acceleration at sea level
I_{sp}: Specific impulse
J: Generic cost function
L: True longitude
m: Mass
r: Orbit radius
p: Semilatus rectum
T: Thrust
T_p: Prediction horizon
T_s: Sampling time
u: Acceleration
v: Velocity

Acronyms/Abbreviations
ECI: Earth-Centered Inertial
MEOE: Modified Equinoctial Orbital Element
MIMO: Multi-input Multi-Output
MPC: Model Predictive Control
NMPC: Nonlinear Model Predictive Control
S/C: Spacecraft

1. Introduction

Space missions are based, among others, on two fundamental operations. The first one is the mission planning, or guidance, which is typically carried out on-ground by employing the classical astrodynamic methods. The second one is the spacecraft trajectory/orbital control, that, in many cases, is performed in open-loop, with occasional feedback corrections driven by a human agent (see, e.g., [1]). However, the current approach in designing and implementing the guidance and control on space vehicles appears not to be suitable for certain future missions, where the S/C will be required to autonomously perform complex orbital maneuvers, minimizing the human intervention from ground and satisfying many strict mission constraints and requirements [2, 3, 4]. In this framework, MPC appears to be a key technology, capable to provide significant advantages in terms of autonomous guidance and control strategies. These latter are fundamental in view of future space missions. Indeed, the MPC approach can significantly improve the capabilities of the space vehicles to autonomously plan complex maneuvers reducing the effort in designing the mission on ground, a task which is usually carried out by means of the standard astrodynamics open-loop methods. Whereas the classical approach in planning space missions expects a trajectory design to be tracked by employing a controller on board, the MPC approach is able to jointly perform the trajectory planning and control in a unique guidance and control algorithm. Moreover, the MPC is a very flexible approach, able to manage MIMO linear and nonlinear systems, input and state constraints, and to optimize a wide class of cost functions.

In general, MPC applications in space missions are various, involving both linear/linearized and nonlinear dynamics. Over the last years, deep investigations were focused on the proximity operations and the relative motion between a chaser satellite and a target problem during a rendezvous maneuver (see, e.g., [5, 6, 7, 8, 9]). Examples include [10], which presents a MPC strategy for a minimum-propellant rendezvous with a sparse actuation behavior. Other applications are concerned with the formation flight of different satellites, including relative motion between spacecrafts [11], and station keeping [12]. As for the transfer between two (or more) orbits, the dynamics is nonlinear, and its potential linearization may lead to deterioration of the control performances. The nonlinearities (in the system dynamics and/or in possible constraints) can be managed by taking advantage of the Nonlinear MPC features. The latter studies often employ low-thrust propulsion systems (see, e.g., [13, 14, 15]) which offer a significant reduction of propellant expenditure when the orbital transfer time is not a strict requirement. Nevertheless, the cited works are often limited to the case of linear (or linearized) dynamics and constraints, and/or they are mainly focused on autonomous low-thrust strategies.

In this paper, we propose a novel NMPC strategy for autonomous guidance and control in space missions which expect high-thrust maneuvers. The proposed framework introduces two main features: (i) a strong enhancement of the S/C capability in autonomously trajectory planning, reducing the effort in designing the guidance on ground; (ii) the trajectory optimization from the propellant consumption point of view. Indeed, in manned or unmanned mission design, the propellant expenditure usually represents the most important metric [16], leading to the design of different cost functions, with respect to the classical problem for which the MPC was originally conceived, which are based on the 1-norm of the thrust signal, i.e., sparse MPC, (see, e.g. [10, 17, 18, 19, 20]. To this end, we introduce a modified NMPC cost function in order to obtain a sparse-in-time and bang-bang behavior of the control signal. The bang-bang behavior is important in view of high-thrust autonomous guidance, since the S/C engines are allowed to fire only at those points along the orbit, where maneuvering is cheaper, delivering the maximum thrust available without any propellant expensive transient. On the other hand, the sparsity criterion ensures an optimal propellant consumption, avoiding long periods of undesirable low continuous thrust. Furthermore, due to technical limitations of a real propulsion system, the maneuver ΔV budget cannot be delivered in a single infinitesimal-time impulse: gravity and misalignment losses are introduced if not thrust vectoring and ΔV subdivision optimization are performed [21]. The classic astrodynamics methods tackle this problem by subdividing a-priori the maneuver in ``N" finite impulse (see, e.g. [22]) and, afterward, by optimizing the single impulses. Conversely, the strength of the proposed NMPC approach is that both ΔV sub-division and single burns optimizations are nested in a single optimization process.

Another important feature of the proposed NMPC strategy is that the internal prediction model is based on the so-called MEOEs dynamics of the two-body restricted problem. Conversely to the position/velocity dynamics representation, the MEOEs formulation allows us to generate a reference trajectory just by assigning the orbital parameters, without specifying the S/C position along the orbit and avoiding the significant numerical singularities affecting the Keplerian orbital elements. As a case study, the proposed methodology has been employed for a non-coplanar LEO-GEO transfer, highlighting the differences in algorithm design and in mission performances with respect to the other classical astrodynamic approaches.

The paper is organized as follows. In Section 2, the S/C nonlinear dynamics is described by means of the MEOEs variational equations. In Section 3, the NMPC framework is presented. The case study is treated in Sections 4 and 5. In particular, the orbital transfer strategies and the NMPC algorithm are discussed in Section 4 and the relevant results are shown in Section 5. The conclusions are drawn in Section 6.

2. Spacecraft Dynamics

Consider the two-body equation for a S/C of mass m_1, orbiting around a main body of mass m_2, where $m_2 \gg m_1$. The equation is the following:

$$\dot{r} = -\frac{\mu r}{\|r\|_2^3} + \frac{T+F}{m_1} \tag{1}$$

where r is the S/C position in ECI J2000 inertial reference frame, T is the thrust delivered by the engines, and F is the sum of all non-Keplerian perturbations. The orbital dynamics may be also uniquely described by means of a set of six independent elements. The most common parametrization consists in describing the S/C state by means of the so-called Keplerian orbital elements. Nevertheless, this set suffers from singularities when the orbit is circular (i.e., the eccentricity is null) and/or equatorial (i.e., the inclination is null). Several alternative parametrizations are available such that the singularities are mitigated or completely avoided. One of these alternatives is given by the MEOE set $\zeta = [p, \eta, \sigma, h, k, L]^T$ (see, e.g. [23]). Note that, η, σ are the components of the eccentricity vector projected onto the equinoctial reference frame, whilst h, k are the projection of ascending node vector onto the equinoctial reference frame. The MEOE set suffers from singularities only in the rare case of retrograde equatorial or parabolic orbits. An alternative formulation to make this set completely non-singular has been proposed by [22]. The map between the position/velocity and Keplerian and/or MEOEs is well described in [24]. In formulae, the S/C dynamics in terms of MEOEs reads:

$$\dot{\zeta} = b(\zeta) + \boldsymbol{G}(\zeta)u. \tag{2}$$

The complete S/C dynamics in terms of MEOEs is quite complex and it will be omitted in this paper. The full S/C nonlinear dynamic model in terms of MEOEs can be found in [17]. Note that, $u = [u_R, u_T, u_N]^T$

represents the non-inertial acceleration vector (i.e., non-Keplerian plus thrusting contributes) in radial, tangential, and normal directions, respectively, according to the Frenet-Serret reference frame. The radial direction is positive when pointing away from the Earth's center, the tangential direction along the direction of the orbital motion, and the normal direction completes the right-handed reference frame.

An important ingredient to add to the state equations is the satellite mass variation due to the engine activity during the maneuvers. The variation is accountable by taking into account the following equation:

$$\dot{m} = \frac{\|T\|_q}{I_{sp} g_0} \tag{3}$$

where $\|\cdot\|_q$ represents a suitable vector norm depending on the engine mounting configuration. In aerospace applications, the q-norm is intrinsically related to the engine mounting configuration. Indeed, the 1-norm and the 2-norm are representative of orthogonal engines mounted on each side of the spacecraft and a steering main engine configuration mounted only on one side of the spacecraft, respectively (see, e.g., [10] and [16]).

In summary, the S/C dynamics consists of a nonlinear MIMO system where the state is $x = [\zeta, m]^T \in \mathbb{R}^7$ and the input is $u = [u_R, u_T, u_N]^T \in \mathbb{R}^3$. The first five states describe the orbit shape and orientation, the true longitude L describes the S/C position along the orbit, and the last one the mass variation due to the engine activity. Note that, when gravity is the only force acting on the S/C, $\dot{p} = \dot{\eta} = \dot{\sigma} = \dot{h} = \dot{k} = 0$, while L changes. Conversely to the position-velocity formulation of S/C dynamics, the orbital parameters grant the possibility of defining a target orbit without specifying its position along the orbit. This latter enhances the flexibility in designing the feedback control law, since only some orbital parameters can be picked as output to be controlled.

3. Nonlinear Model Predictive Control Framework

Consider a nonlinear system in affine-in-the-input form:

$$\dot{x}(t) = f\big(x(t)\big) + g\big(x(t)\big)u(t) \tag{4}$$

where $x \in \mathbb{R}^{n_x}$ and $u \in \mathbb{R}^{n_u}$ are the state and the input, respectively. Note that, in most aerospace applications, the satellite dynamics is in this affine-in-the-input form. Examples include the case of two-body motion approximation, the Gaussian variational formulation of the Keplerian orbital elements, and the Clohessy-Wiltshire equations [25].

We assume that the state is measured in real-time, with a sampling time T_s. If this assumption does not hold, an observer can be employed. The measurements are $x(t_k), t_k = T_s k, k = 0, 1, \dots$. At each time $t = t_k$, a prediction of the system state and output over the time interval $\left[t, t + T_p\right]$ is performed, where $T_p \geq T_s$ is the prediction horizon. The prediction is obtained by integrating (4). At any time $\tau \in \left[t, t + T_p\right]$, the predicted state $\hat{x}(\tau)$ is a function of the 'initial' state $x(t)$ and the input signal, whereas $u(t\colon\tau)$ denotes the input signal in the interval $[t, \tau]$. At each time $t = t_k$, we look for an input signal $u^*(t\colon\tau)$, such that the prediction $\hat{x}\big(\tau, x(t), u^*(t\colon\tau)\big) \equiv \hat{x}\big(u^*(t\colon\tau)\big)$ has the desired behaviour for $\tau \in \left[t, t + T_p\right]$. Mathematically, at each $t = t_k$, the following optimization problem is solved:

$$\begin{aligned} & u^*\big(t\colon t + T_p\big) = \arg\min_{u(\cdot)} J\left(u\big(t\colon t + T_p\big)\right) \\ & \text{subject to:} \\ & \dot{\hat{x}}(\tau) = f\big(\hat{x}(\tau), u(\tau)\big), \quad \hat{x}(t) = x(t) \\ & \hat{x}(\tau) \in X_C,\ u(\tau) \in U_C. \end{aligned} \tag{5}$$

X_C and U_C are suitable sets describing possible constraints on the state and input respectively. A receding control horizon strategy is employed: at a given time $t = t_k$, only the first optimal input is applied to the plant, and the remainder of the solution is discarded. Then, the complete procedure is repeated at the next time $t = t_{k+1}$.

In this paper, we focus on studying a minimum-propellant $\mathcal{L}_1 \backslash \mathcal{L}_2^2$ cost function:

$$\begin{aligned} J\left(u\big(t\colon t + T_p\big)\right) = \int_t^{t+T_p} \|\tilde{x}_P(\tau)\|_Q^2 + \|\boldsymbol{R}u(\tau)\|_q \, \mathrm{d}\tau \\ + \left\|\tilde{x}_P\big(t + T_p\big)\right\|_P^2. \end{aligned} \tag{6}$$

The $\|x\|_W^2$ notation represents the (square) weighted norm of a vector $x \in \mathbb{R}^n$ such that $\|x\|_W^2 \doteq x^T \boldsymbol{W} x = \sum_{i=i}^n w_i x_i^2$ and $\boldsymbol{W} = \operatorname{diag}(w_1, \dots, w_n) \in \mathbb{R}^n$, $w_i \geq 0$. The predicted tracking error is $\tilde{x}_P(\tau) = r(\tau) - \hat{x}(\tau)$, whereas $r(\tau)$ is the desired reference to track and $\hat{x}(\tau)$ is obtained by integration of (4). The weights $\boldsymbol{Q} \geq 0, \boldsymbol{P} \geq 0$, and $\boldsymbol{R} > 0$ are diagonal matrices. Note that $\boldsymbol{Q}, \boldsymbol{P} \in \mathbb{R}^{n_x \times n_x}$ and $\boldsymbol{R} \in \mathbb{R}^{n_u \times n_u}$. Note also that, the term relevant to the command input in (6) is a weighted $\mathcal{L}_1$ norm.

4. Non-coplanar LEO-GEO Transfer Strategies

The LEO-GEO transfer is one of the most common space maneuvers: it is widely exploited for placing artificial satellites (telecommunications, weather forecasts, etc.). Due to its large importance, aerospace research is still focusing on designing optimized non-coplanar GTO. In general, the transfer among coplanar orbits has been deeply investigated over the last years and several guidance analytical solutions are available (see, e.g., [26, 27]). Indeed, if the coplanar GTO transfer has an analytical (and trivial) minimum-propellant optimal solution (i.e., the Hohmann transfer), the out-of-plane GTO has not an exact optimal solution and many strategies can be explored and are available in literature. Straightforwardly, if a satellite is not launched from an equatorial space center, the latitude of the launch site must be corrected during the GEO injection in order to nullify the inclination offset. To sum up, the co-planar GTO is a quite rare case and represents an `abstraction', whereas the non-coplanar case is worthier of interest.

Within this framework, the NMPC-based guidance and control appears to be a suitable technology for optimizing the propellant expenditure and enhancing the S/C autonomy. Indeed, we can identify some main areas of interest in which the NMPC is able to mitigate the critical issues arising during an out-of-plane GTO.

First of all, the overall ΔV budget involved in these kinds of missions goes approximately from 3.5 km/s up to 5 km/s, depending on the radius and the inclination of the starting orbit. Clearly, due to the technical limitation of the engines, the maneuver sub-division into two different burns (one for GTO injection and one for GEO injection) leads to the introduction of misalignment and gravity losses with a consequential ΔV increment and non-optimal propellant expenditure. Indeed, since the ΔV cannot be delivered instantaneously, the finite-burn will not take place exactly at the apses. This phenomenon takes the name of `gravity losses' which are accountable as

$$\Delta V_{GL} = \int_{t}^{t+\Delta t} g_i \sin\gamma \; dt \tag{7}$$

where Δt is the time span of engines ignition and g_i the generic gravity acceleration. Clearly, if maneuvering at the apses, where $\gamma = 0$, ΔV_{GL} is null. Therefore, in order to nullify the integral in (7), the burn must occur in an infinitesimal time interval. This is in contrast with the technological limitation of the real propulsion systems, making the impulsive burn to be unfeasible. Furthermore, as discussed by [21], the ΔV increasing during a finite-time maneuver is also due to the non-constant thrust direction during the burns leading also to poor accuracy in tracking the reference orbit. This latter effect is intrinsically related to the so-called misalignment losses, introduced when the thrust direction is not parallel at the osculating S/C velocity. To sum up, when the ΔV budget is too huge to be delivered in a single burn, an N-impulse sub-division of the maneuver is required.

Furthermore, a second issue can be represented by the optimization of each N-th burn of the transfer. Indeed, once the `N' number of the burns is available, we still do not know neither how much ΔV should be allocated for each burn nor the direction of the burn itself. This issue is emphasized by the necessity of combining the orbit shape change with the orbital plane change.

Finally, once the guidance algorithm has identified the `N'-impulse sub-division of the maneuver and each burn has been optimized in terms of ΔV allocation and direction of the burn, a suitable control system has to track the reference signal coming from the guidance.

In general, the NMPC-based guidance and control is able to tackle the mentioned issues, nesting all the optimization and control tasks into a unique algorithm. Moreover, the on-line optimization process allows the S/C to adapt to external disturbances and enhances the level of autonomy.

The non-coplanar LEO-GEO transfer is not a trivial problem to solve, also when assuming - as we do in the work - that the starting and the final orbit are circular: only approximate (and sub-optimal) solutions are available in literature. A first preliminary (but expensive and ideal) strategy consists in performing a three-burns mission: two burns for the Hohmann's transfer and the last one for the inclination offset. When adopting this strategy, in order to reduce the ΔV related to the inclination change, which is proportional to the spacecraft orbital tangential velocity, the inclination offset can be nullified once the final GEO altitude has been achieved.

Another interesting - but still impulsive and ideal - strategy consists in the four-burns bi-elliptic (or Sternfeld's) transfer. In general, the bi-elliptic maneuver is the most efficient coplanar transfer when the radius ratio between the initial and the final circular orbits is greater than 11.94. Nevertheless, for the non-coplanar case, one can take advantage in nullify the inclination offset when the S/C is at the apoapsis of the supporting ellipse, at the farthest point from the attractor. Ideally, if the apoapsis of the supporting ellipse coincides with the border of the main body sphere of influence, at that point, the ΔV relevant to inclination change is null.

However, both the Hohmann's transfer and the bi-elliptic strategy provide a simple analytical ΔV budget that does not take into account the possibility of combining the inclination change with the semi-major axis change maneuver. Then, the propellant expenditure for performing these two strategies is higher with respect to the combined maneuvers. Moreover, no `N'-impulse sub-division of the burn is expected, letting the real ΔV budget be higher because of the gravity and misalignment losses.

In modern astrodynamics, there are several and efficient strategies for performing an optimal non-coplanar LEO-GEO transfer. A strategy is widely discussed by [28]. A way to reduce the maneuver ΔV is to sub-divide the inclination changes into two different burns: a fraction of the inclination offset is corrected during the GTO injection maneuver and the remaining during the GEO injection. In detail, [28] proposes an approximate analytical expression for the optimal value of the first inclination correction. Nevertheless, this approach suffers from two main criticalities: i) the solution of the optimal inclination sub-division does not provide the direction of the burn, which is available by solving the Lambert's problem; ii) the maneuvers are still considered impulsive, and then, they do not account for the extra ΔV budget - as in a real space scenario - neglected by the impulsive approximation.

A different strategy is proposed by [29]. The authors take advantage of the Lawden's primer vector theory for optimizing the non-coplanar transfer. This methodology offers the great benefit of skipping the Lambert's problem solution since the Pontryagin-based optimization problem provides the unit vector of the optimal direction of the burn. Nevertheless, also in this case, the orbital transfer is dealt as a combination of impulsive maneuver, being the ΔV losses not accounted in the overall budget. Moreover, conversely to the NMPC strategy, both [28, 29] propose an off-line optimization, being not robust to neglect orbital perturbations and sensors/actuators disturbances.

4.1 NMPC Approach and Design

As pointed out above, the core of the work is to design and test the capability of an autonomous - closed loop - system able to perform a non-coplanar orbital transfer without any human feedback correction during the mission, guaranteeing, at the same time, a high performance in terms of propellant expenditure and reference tracking. In this context, the NMPC appears to be a promising technology: it can nest into a single optimization algorithm the guidance and control sub-systems. To sum up, the following critical issues must be accounted for the design phase:

- The `N'-impulse sub-division of the maneuver.
- The amount of ΔV allocated for each burn.
- The direction of the burns.
- The tracking of the final reference orbit.

To this end, a modified NMPC cost function (see (6)) is employed in order to have a sparse thrust profile and a bang-bang behavior: (i) the sparsity of the controller avoids a continuous and undesirable thrust activity away from the apses/nodes, leading to sub-optimal fuel consumption; (ii) the bang-bang profile allows to concentrate the maximum thrust possible when the S/C is at apses/nodes, reducing the gravity losses in (7). The 1-NMPC and 2-NMPC (depending on $q = 1, 2$ in the $\|\boldsymbol{R}u(\tau)\|_q$ term of (6)) configurations have been considered.

Remark. For non-coplanar Hohmann transfers (and in general for non-coplanar but coaxial orbital transfers), the most efficient way to maneuver is to combine in a single burn the change in semi-major axis with the change in inclination. This is a trivial notion resulting from the Carnot's law. Furthermore, since we are dealing with circular orbits transfer, the apses are not uniquely defined. This allows to consider the line of nodes to be coincident with the apses line. Then, in order to obtain a suitable combination of semi-major axis/eccentricity and inclination changes, the intersections between the initial and the reference orbits (i.e., the ascending and descending nodes) are considered as the maneuver points.

In this work, we adopt the strategy drawn in Figure 1. The mission is subdivided into two consecutive phases: the GTO injection and the GEO injection. On the left-hand side, the GTO injection maneuvers are represented (top view and side view respectively). On the right-hand side the GEO injection maneuvers are sketched (top view and side view respectively). Note that, the final GEO orbit is not drawn. The dashed line represents the line of nodes that coincides with the apses line. This latter lies on the Earth's equatorial plane. During the first phase (the GTO injection) we do not perform any inclination offset correction. In detail, the S/C fires at the perigee (point A) until - after many revolutions - it reaches the GEO radius when at apogee (point C), being $\overline{AB} = r_{LEO} + r_{GEO}$ the GTO semi-major axis. When performing the second phase (GEO injection), the S/C maneuvers at the GTO apogee (point C), changing, at the same time, the orbit inclination and its perigee (points A', A'', ..., $A^{(n)}$) until the S/C angular momentum is parallel with the $\hat{z}_{ECI}$ unit vector and the orbital radius in $A^{(n)}$ is equal to r_{GEO}.

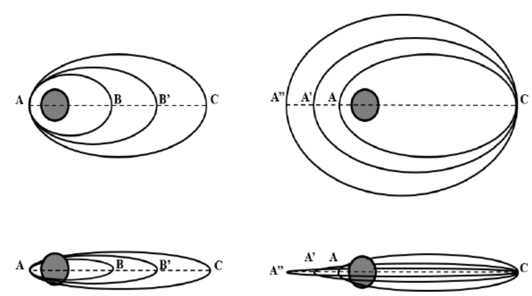

Fig. 1. Orbital Transfer Scheme

4.2 Guidance and Control Architecture

One of the keys and innovative points of the guidance and control architecture is the subdivision of the control system into two inner NMPC loops:

- $NMPC_S$ loop, handling the S/C altitude and eccentricity
- $NMPC_O$ loop handing the S/C orbit orientation.

From the equinoctial elements point of view, the guidance and control system is decoupled into two different loops sharing the same plant but with different outputs and inputs. The NMPC overall architecture is sketched in Figure 2 In detail we have:

- $NMPC_S$:
    - The state $x = [\zeta, m]^T$.
    - The output $y_S = [p, \eta, \sigma]^T$.
    - The input $u_S = [u_R, u_T]^T$.

- $NMPC_O$:
  - The state $x = [\zeta, m]^T$.
  - The output $y_O = [h, k]^T$.
  - The input $u_O = u_N$.

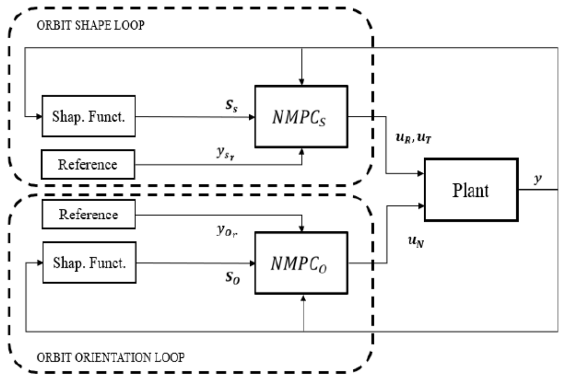

Fig. 2. Guidance and Control Architecture

Even though the system is not perfectly decouplable, this choice is aimed to split the required maneuver in order to obtain a low computational complexity of the algorithm and, at the same time, to guarantee high reference tracking performances. Note also that, even though the $NMPC_S$ handles the radial component of the thrust acceleration, this latter is often neglected since not required for semi-major axis/inclination changes.

Since the two NMPC loops are not independent of each other, the contribution of $NMPC_S$ leads to different behavior of the plant with respect to the one predicted during the optimization phase of $NMPC_O$, and vice versa. In other words, the effect that an NMPC determines on the system can be seen by the other as an additional disturbance on the plant. The addition of this disturbance does not, however, result in any change in the model used within the optimization algorithm to predict the future behavior of the system. This latter is due to a fundamental property of the NMPC: the inherent robustness.

4.3 Enforced Guidance and Shaping Functions

Tuning of the NMPC parameters is one of the most critical issues in designing the guidance and control system, in particular, the prediction horizon T_p and the $\boldsymbol{R}$, $\boldsymbol{P}$ and $\boldsymbol{Q}$ matrices. The prediction horizon allows to define for how long time in the future the system is predicted and optimized. Indeed, a long prediction interval enhances the closed-loop stability of the system. However, this results in less accuracy in short-time tracking. In the framework of space high-thrust missions, the choice of T_p is a crucial issue. Indeed, when dealing with these kinds of space missions, every single maneuver is characterized by burns lasting tens of seconds (or a few minutes). On the other hand, the characteristic time of the orbital motion - especially when dealing with GTO - is in the order of many hours. Therefore, the prediction horizon should be enough large to predict the S/C behavior along the orbit and, at the same time, enough short for guaranteeing great accuracy during the short-time burns. In this work, we choose a value of tens of seconds for the prediction horizon. This value is much lower than the involved orbital periods, but it is comparable to the time required to perform the burns. This allows to promote the sparse behavior of the controller and to increase the short-time tracking accuracy.

A novel methodology for dealing with long-time accuracy is the design of an enforced guidance by varying the entries of the weighting matrices during the mission. The matrices are tuned in order to obtain a suitable trade-off between convergence time ($\boldsymbol{P}$ and $\boldsymbol{Q}$ matrices) and fuel consumption $\boldsymbol{R}$ matrix).

Remark. In our NMPC strategy, $\boldsymbol{P}$ and $\boldsymbol{Q}$ are time-varying matrices. Their values are adapted on-line according to proper shaping functions, which increase or decrease depending on the S/C position on the orbit. The closer it is to the maneuver point, the more $\boldsymbol{P}$ and $\boldsymbol{Q}$ increase. This methodology assists the NMPC in the`N'-burn sub-division of the maneuver. The choice is aimed to enforce the guidance, especially when using a short prediction horizon, and to reduce the computational complexity.

As previously mentioned, an innovative feature in the developed framework is the presence of an enhanced guidance with takes advantage of the so-called "Shaping Function" whose output is defined as S_f. These functions are used to support the NMPC in splitting the total maneuver into 'N'-impulses. Indeed, due to the short prediction horizon, the NMPC is not always able to predict exactly where it is cheaper (from a fuel expenditure point of view) to maneuver. Of course, there are several methods to enforce the guidance. For example, an alternative approach would consist in using of an additional `outer' NMPC with much higher sampling and prediction times to form a hierarchical architecture. In this way, the NMPC in the outer loop would have the task to optimize the guidance and planning the `N'-impulse structure, while the two inner NMPC loops would handle the burns of each maneuver. However, this approach would have entailed both great complexity in the architecture and higher computational costs. For this reason, the on-line adaptation of the NMPC parameters has been chosen.

Define with θ the S/C true anomaly, changing instant by instant according to the satellite position during the orbital transfer. The idea of the algorithm is to exploit the knowledge of the satellite position (at each instant) for computing a function that takes the maximum value when this position coincides with one of the two nodes. In order to discern the ascending from the descending node, it is necessary to define the one in which to maneuver. Considering a prograde orbit, we chose the ascending node for the enlarging of the orbit radius and the descending node (which will coincide with the apoapsis) for the eccentricity/inclination change. Therefore, the orbit is subdivided into two quadrants according to the θ value: ascending node section for $\theta \in \left[-\frac{\pi}{2}, \frac{\pi}{2}\right]$, and descending node portion for $\theta \in \left[-\pi, -\frac{\pi}{2}\right] \cup \left[\frac{\pi}{2}, \pi\right]$. Then, when the satellite is not required to maneuver, the shaping function output S_f is always null.

Therefore, we take advantage of the following notion: during a co-axial orbit transfer, the direction of the line of nodes keeps constant, that, in this particular application coincides with the apses line. We remind that the equinoctial parameters h, k are the line of nodes projections onto the equinoctial plane and then the line of nodes direction is determined as $\hat{n} = \frac{[h,k]}{||[h,k]||_2}$. Therefore, considering r_{EQ} as the S/C position in the equinoctial reference frame, a suitable condition for engines ignition is that the cross product $\left|\left|\hat{n} \times \hat{r}_{EQ}\right|\right|_2 = 0$. Then, the Shaping Function output is defined as

$$S_f = \left(\cos\left|\left|\hat{n} \times \hat{r}_{EQ}\right|\right|_2\right)^A \qquad (7)$$

Note that, this cosine in (7) is not meant as a trigonometric function, but it is used to obtain a bell-shaped function whose peak is reached when r_{EQ} is parallel to the line of nodes. In the other cases, since the $\left|\left|\hat{n} \times \hat{r}_{EQ}\right|\right|_2$ is always in the range $(0,1]$, the cosine function will take values smaller than its maximum. Finally, the A parameter determines the steepness of the function.

Remark. The crucial difference between the proposed approach and the classical optimization guidance methods presented by the previously cited works consists in how and when the trajectory optimization is performed. Indeed, whereas the classical orbital optimization works are based on off-line trajectory design and the derived results are useful for the guidance task only, the proposed NMPC approach performs an on-line optimal guidance design and is able to jointly provide the control action needed to track the designed trajectory. This aspect allows the satellite to be robust and flexible with respect to sudden disturbances, constraints, and neglected perturbations that may arise during a GTO. It also enhances the autonomy of the spacecraft in accomplishing different complex maneuvers.

5. Simulation Results

The proposed NMPC strategy has been evaluated on a non-coplanar LEO-GEO orbital transfer. The S/C is deployed into a LEO orbit with an initial radius of 7192 km, an eccentricity of 0, and an inclination of 12.85°. The target orbit is characterized by an altitude of 42168 km, an eccentricity equal to 0, and an inclination of 0°.

The corresponding MEOEs of the initial and the reference orbits are reported in Table 1.

Table 1. Orbital parameters

	$p\ [km]$	η	σ	h	k
LEO	7192	0	0.224	-0.932	-2.2
GEO	42168	0	0	0	0

The trajectory of the spacecraft is subjected both to state and input nonlinear constraints. In the example scenario, we design a safety sphere around the Earth (in order to avoid possible satellite/Earth collisions or atmosphere re-entries) with a radius of $1.5\ r_E$ where $r_E = 6378.1\ km$ is the Earth radius. Therefore, the admissible state set is defined as:

$$X_C = \left\{x(t) \in \mathbb{R}^6 : 1.5\ r_E - \left|\left|r(t)\right|\right|_2 \leq 0, \forall t\right\} \qquad (8)$$

Concerning the input constraint, we point out that each NMPC has $1\ kN$ of thrust authority. Then, according to the level of the required thrusting force, the S/C is equipped with high-trust chemical engines. Table 2 summarizes the constant values of the orbital simulator and the engine parameters. Finally, the NMPC and Shaping Function design parameters are listed in Tables 3 and 4. The orbital simulator and the guidance and control algorithms have been implemented in a Matlab/Simulink environment, moreover, the optimization problem has been dealt with Sequential Quadratic Programming solver provided by the Matlab Optimization Toolbox.

Table 2. Simulation and propulsion parameters

Description	Value
Earth Planetary Constant	$398600.442\ km^3 s^{-2}$
Earth Gravity Accelaration	$9.807\ ms^{-2}$
Earth Mean Radius	$6378.1\ km$
Engine Specific Impulse	$375\ s$
Maximum Thrust	$1\ kN$
S/C wet mass	$2000\ kg$

Table 3. NMPCs parameters

Description	Value
T_S	$1\ s$
T_p	$30\ s$
$\boldsymbol{R}$	$100\ \boldsymbol{I}_{2\times 2}$

$\boldsymbol{Q}$	$S_f\ diag(10,1,1)$
$\boldsymbol{P}$	$S_f\ diag(100,10000,10000)$
A	10000

Table 4. NMPCo parameters

Description	Value
T_S	$1\ s$
T_p	$30\ s$
$\boldsymbol{R}$	100
$\boldsymbol{Q}$	$50S_f\ \boldsymbol{I}_{2\times2}$
$\boldsymbol{P}$	$5000S_f\ \boldsymbol{I}_{2\times2}$
A	10000

In Figures 3-4, the resulting trajectory out-coming from the simulation campaign is presented in two different views. It can be seen that the eccentricity and inclination changes are combined in a single maneuver at the apogee of the GTO orbit, resulting in a reduction of the ΔV budget. Note that, in Figures 3-4, only the 1-NMPC orbital path has been plotted, since the 2-NMPC case slightly differs in terms of performance and then, the discrepancies between the two orbital trajectories are not visible on large scale. The proposed NMPC strategy is able to autonomously design the whole mission, splitting the total ΔV in optimal sub-portions. This results in a LEO-GEO transfer consisting of multiple revolutions, in which the required maneuvers are applied only nearby the perigee of the inner orbit or the apogee of the outer orbit. Hence, the system is capable of autonomously detecting that, due to the technological limitations of the real propulsion systems, the overall ΔV budget cannot be delivered in a single maneuver. Then, the required change in velocity is divided into suitable, multiple and small ΔVs applied at the apses, where the gravity losses are small, and for short time intervals. This is the empirical demonstration of how the functionality of NMPC-based autonomous guidance and control is a suitable methodology for dealing with high-thrust space missions.

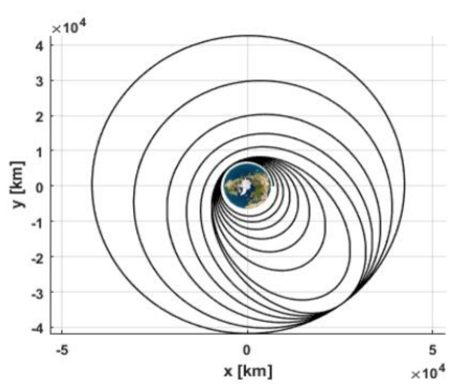

Fig. 3. LEO-GEO NMPC trajectory for altitude-eccentricity changes

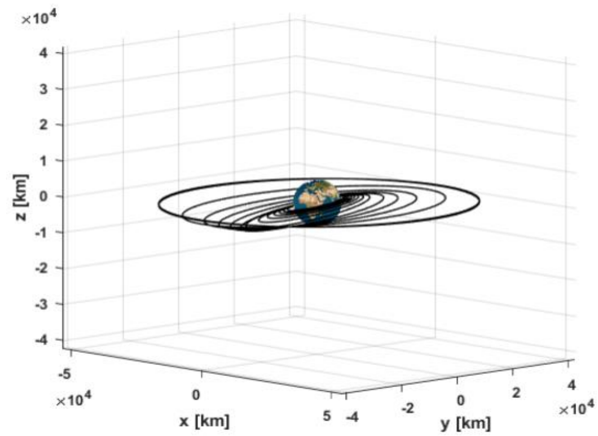

Fig. 4. LEO-GEO NMPC trajectory for inclination changes

It should be also recalled that, in a real mission analysis scenario, the high-thrust GTO can be designed, through the classic, but not optimal, astrodynamic approaches, by sub-dividing the ΔV budget in order to perform multiple revolutions. This strategy expects a considerable effort in optimization and design on ground, generally by iteratively solving a two-point boundary value problem and then employing a controller for the trajectory tracking. The main difference between the classic astrodynamic methods and the proposed NMPC framework is the NMPC capability to incorporate in a unique algorithm the guidance and the control systems, autonomously sub-dividing the maneuvers into shorter portions. Then, the novelty is the autonomous replication of these kinds of strategies with a strong reduction in mission design effort and mission analysis verification effort, and above all, better performances in terms of fuel consumption and ΔV budget with respect to the Hohmann and bi-elliptic strategies.

The performance features of the proposed strategies (i.e., non-optimized Hohmann transfer, bi-elliptic transfer, 1-NMPC, and 2-NMPC) are summarized and compared in Table 5. For the bi-elliptic case, the apogee radius of the supporting ellipse has been considered equal to 4.2168e4 km.

Table 5. Orbital parameters

Configuration	Fuel cons. [kg]	ΔV [km/s]
Hohmann	1393.7	4.389
Bi-elliptical	1386	4.343
1-NMPC	1317.3	3.953
2-NMPC	1316.9	3.950

As highlighted in Table 5, the NMPC configurations are able to provide better solutions in terms of fuel consumption with respect to the two ideal methods, also obtaining satisfactory performance as far as the normalized tracking error. The results demonstrate the benefits of using the novel NMPC strategy for quasi-impulsive maneuvering applications both from the designing effort and the performance point of views. The performances efficiency is mainly due to the use of the mixed $\mathcal{L}_1 - \mathcal{L}_2^2$ functional, which leads to a sparser control input and in a bang-bang thrust behavior.

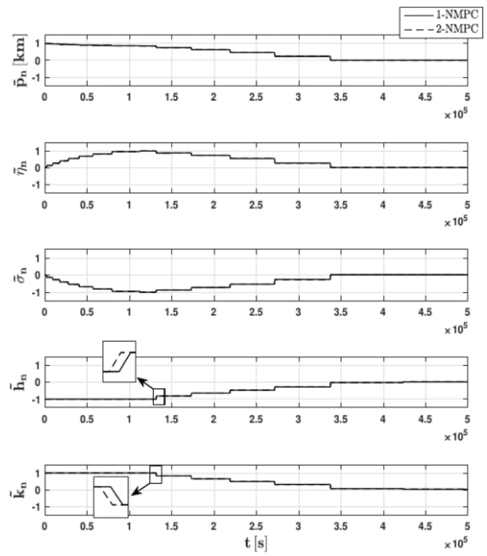

Fig. 5. MEOEs Normalize Tracking Error

Figure 5 shows the evolution of the normalized tracking error on the output MEOEs variables. As already highlighted in Table 5, the NMPC strategies return a great accuracy in tracking the reference GEO trajectory.

Figure 6 shows the tracking error of the most involved parameters in this kind of orbital transfer, i.e., altitude a, eccentricity e, inclination i, and the orbital radius r.

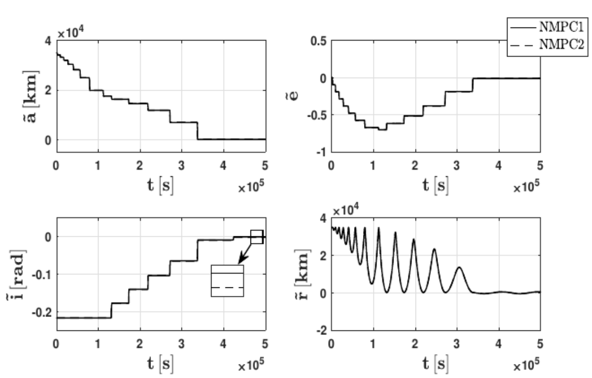

Fig. 6. Keplerian parameters Tracking Error

In Figure 7, the normalized tangential and normal thrust components of the 2-NMPC and 1-NMPC are displayed (we remind that the radial component is useless in the example scenario). The bang-bang control promotes the generation of an input signal which can assume only three states: maximum, minimum, and zero. The transition between states occurs in infinitesimal time.

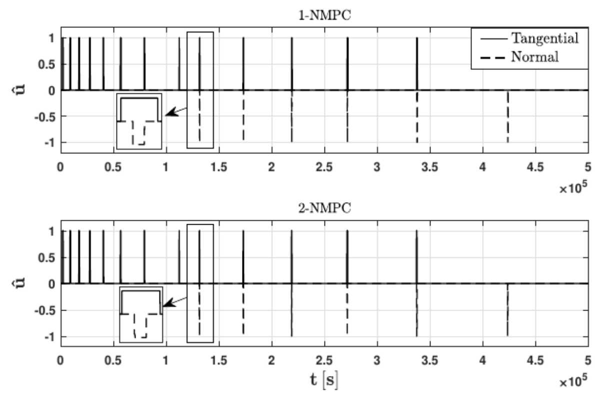

Fig. 7. Command activities comparison

6. Conclusions

The paper proposes a novel NMPC strategy for guidance and control design in autonomous high-thrust space missions. The methodology promotes a sparse-in-time behavior and a bang-bang profile of the optimal control input. The standard NMPC cost function has been modified by substituting the quadratic term of the input with the signal 1-norm and comparing the performances of the vector 1-norm and 2-norm representing different engines mounting configurations. Indeed, the standard quadratic configuration may result in a continuous command activity, leading to sub-optimal fuel efficiency. This drawback is tackled by proposing an alternative approach based on a bang-bang control behavior and a sparse-in-time input signal, which are the desirable properties for achieving the optimum propellant consumption. These key points have been empirically proved with a LEO-GEO transfer simulated example. The proposed methodology output is the autonomous ΔV budget subdivision into multiple firing, such that the propulsion system is switched-on only nearby those points where maneuvering is cheaper, for short time intervals. This approach has been implemented and tested for a non-coplanar LEO-GEO transfer and the results have been compared with some classical - but not optimal - astrodynamics approaches. The obtained results show how the proposed NMPC strategy can be suitable for autonomous high-thrust space missions, ensuring propellant minimization and a high level of autonomy.

References

[1] L. Lu, H. Li, W. Zhou, J. Liu, Three-impulse point return orbit design for manned lunar high-latitude exploration mission, Acta Astronautica, 179 (2021) 88-98.

[2] R. Shi, T. Long, H. Baoyin, Multi-fidelity and multi-objective optimization of low-thrust transfers with control strategy for all-electric geostationary satellites, Acta Astronautica, 177 (2020) 577-587.

[3] M. Pontani, M. Pustorino, Nonlinear Earth orbit control using low-thrust propulsion, Acta Astronautica, 179 (2021) 296-310.

[4] Y. Chihabi, S. Ulrich, Hybrid Guardian Map-based adaptive control of spacecraft formation flying on highly elliptical orbits in the restricted three-body problem, Acta Astronautica, 180 (2021) 370-385.

[5] E.N. Hartley, A Tutorial on Model Predictive Control for Spacecraft Rendezvous, Proceedings of the European Control Conference, 15-17 July 2015.

[6] R. Vazquez, F. Gavilan, E.F. Camacho, Model Predictive Control for Spacecraft Rendezvous in Elliptical Orbits with On/Off Thrusters, IFAC-PapersOnLine, Vol. 48, Issue 9, pp. 251-256, 2015.

[7] E.N. Hartley, M. Gallieri, J.M. Maciejowski, Terminal Spacecraft rendezvous and capture with LASSO model predictive control, International Journal of Control, Vol. 86, No. 11, pp. 2104-2113, 2011.

[8] M. Leomanni, E. Rogers, S.B. Gabriel, Explicit Model Predictive Control Approach for Low-thrust Spacecraft Proximity Operations, Journal of Guidance, Control, and Dynamics, Vol. 37, No. 6, pp. 1780-1790, 2014.

[9] C. Zagaris, H. Park, J. Virgili-Llop, R. Zappula II, M. Romano, I. Kolmanovsky, Spacecraft Relative Motion with Convexified Keep-out-Zone Constraints, Journal of Guidance, Control, and Dynamics, Vol. 41, No. 9, pp. 1-9, 2018.

[10] M. Leomanni, G. Bianchini, A. Garulli, A. Giannitrapani, R. Quartullo, Sum-of-norms Model Predictive Control for Spacecraft Maneuvering, IEEE Control Systems Letters, Vol. 3, No. 3, pp. 649 - 654, July 2019.

[11] A. Weiss, I. Kolmanovsky, M. Baldwin, R.S. Erwin, Model Predictive Control of Three Dimensional Spacecraft Relative Motion, Proceedings of the American Control Conference, 27-29 June 2012.

[12] A. Weiss, U.V. Kalabic, S. Di Cairano, Station Keeping and Momentum Management of Low-thrust Satellites using MPC, Aerospace Science and Technology, Vol. 76, May 2018, pp. 229–241.

[13] A. Starek, I.V. Kolmanovsky, Nonlinear Model Predictive Control Strategy for Low Thrust Spacecraft Missions, Optimal Control Applications and Methods, Vol. 35, Issue 1, pp. 1-20, 2014.

[14] J.A. Starek, I.V. Kolmanovsky, Model predictive feedback control strategy for low thrust spacecraft interplanetary missions, Advances in the Astronautical Sciences, Vol. 140, January 2011, pp. 1879-1898.

[15] J.J. Arrieta-Camacho, L.T. Biegler, Real Time Optimal Guidance of Low-thrust Spacecraft: An Applications of Nonlinear Model Predictive Control, Annals of the New York Academy of Science, Vol. 1065, January 2006, pp. 174-188.

[16] I.M. Ross, How to Find Minimum-fuel Controllers, Proceedings of the AIAA Guidance, Navigation, and Control Conference and Exhibit, 15-19 August 2004.

[17] M. Pagone, M. Boggio, C. Novara, L. Massotti, S. Vidano, A Sparse Nonlinear Model Predictive Control for Autonomous Space Missions, Proceedings of the 71st International Astronautical Congress, 2020.

[18] S.K. Pakazad, H. Ohlsson, L. Ljung, Sparse control using sum-of-norms regularized model predictive control, Proceedings of the 52nd IEEE Conference on Decision and Control, pp. 5758-5763, 2013.

[19] H. Ohlsson, L. Ljung, Trajectory generation using sum-of-norms regularization, Proceedings of the 49th IEEE Conference on Decision and Control, pp. 540-545, December 15-17, 2010.

[20] M. Pagone, M. Boggio, C. Novara, S. Vidano, A Pontryagin-based NMPC approach for autonomous rendez-vous proximity operations, IEEE Aerospace Conference Proceedings, 2021, 2021-March, 9438226.

[21] H.M. Robbins, An Analytical Study of the Impulsive Approximation, AIAA Journal, Vol. 4, No. 8, 1966.

[22] P.V. Anderson, H. Schaub, \emph{N}-Impulse Formation Flying Feedback Control Using Nonsingular Element Description, Journal of Guidance, Control, and Dynamics, Vol. 37, No. 2, pp. 540-548, 2014.

[23] E.A. Roth, The Gaussian form of the variation-of-parameter equations formulated in equinoctial elements - Applications: Airdrag and radiation pressure, Acta Astronautica, Vol. 12, Issue 10, pp. 719-730, 1985.

[24] J.H. Jo, I.K. Park, N. Choe, M. Choi, The Comparison of the Classical Keplerian Orbit Elements, Non-singular Orbital Elements (equinoctial elements), and the Cartesian State Variable in Lagrange Planetary Equations with J2 Perturbation: Part I, Journal of Astronomy and Space Science, Vol. 28, March 2011, pp. 37-54.

[25] E. Canuto, C. Novara, L. Massotti, D. Carlucci, C. Perez Montenegro, Spacecraft Dynamics and Control: The Embedded Control Approach, Elsevier Aerospace Engineering Series, Oxford, England, UK, 2018, pp. 85-127.

[26] O. Jia-Richards, P.C. Lozano, Analytical guidance for circular orbit transfer with staging of space

propulsion systems, Acta Astronautica, 179 (2021) 69-77.
[27] T. Carter, M. Humi, Two-impulse, bi-parabolic, and bi-elliptical transfers between coplanar elliptical orbits, Acta Astronautica, 177 (2020) 158-171.
[28] D. Grishko, B.O. Vasil'kov, On the Non-coplanar Transfer of Type II between Two Circular Orbits, Russian Aeronautics (IZ VUZ), Vol. 61, July 2018, pp. 355-362.
[29] S. Zaborsky, Geometrical characteristics of optimal transfer between noncoplanar elliptic orbits, Acta Astronautica, Vol. 165, December 2019, pp. 242-247.